Structural biology of starch-degrading enzymes and their regulation

Møller, Marie Sofie; Svensson, Birte

Published in:
Current Opinion in Structural Biology

Link to article, DOI:
10.1016/j.sbi.2016.07.006

Publication date:
2016

Document Version
Peer reviewed version

Structural biology of starch-degrading enzymes and their regulation

Marie Sofie Møller[a,b] and Birte Svensson[a]

Addresses

[a]Enzyme and Protein Chemistry, Department of Systems Biology, Technical University of Denmark, DK-2800 Kgs. Lyngby, Denmark.

[b]Center for Molecular Protein Science, Department of Chemistry, Lund University, 221 00 Lund, Sweden.

Corresponding author: Svensson, Birte (bis@bio.dtu.dk)

Abstract

Starch is a major energy source for all domains of life. Recent advances in structures of starch-degrading enzymes encompass the substrate complex of starch debranching enzyme, the function of surface binding sites in plant isoamylase, details on individual steps in the mechanism of plant disproportionating enzyme and a self-stabilised conformation of amylose accommodated in the active site of plant α-glucosidase. Important inhibitor complexes include a flavonol glycoside, montbretin A, binding at the active site of human pancreatic α-amylase and barley limit dextrinase inhibitor binding to the debranching enzyme, limit dextrinase using a new binding mode for cereal protein inhibitors.

Introduction

Starch is the most abundant storage polyglucan in nature serving as energy source for all domains of life. Accordingly starch degrading enzymes occur ubiquitously in plants, other eukaryotes, bacteria and archaea (see the carbohydrate-active enzymes database, CAZy; [1]). During the biosynthesis starch is deposited as supramolecular, semicrystalline granules basically consisting of two α-glucans, the branched amylopectin and the essentially linear amylose (see [2] for a recent review on starch). In plants starch can be either a transitory energy and building block supply synthesised and degraded in the diurnal cycle in leaves or a long-term storage residing in grains and tubers.

Starch is a simple polymer of α-1,4- and α-1,6-linked glucose residues, yet a multiplicity of enzyme activities is required for degradation of the complex starch granules as well as amylose and amylopectin alone (Figure 1). Starch-degrading enzymes include glycoside hydrolases (GHs), transglycosidases, glycosyl transferases (GTs) (phosphorylases), lyases, phosphatases and lytic polysaccharide monooxygenases (LPMOs). Here emphasis is on enzymes naturally involved in starch degradation, thus bacterial intracellular enzymes acting on glycogen are excluded although they degrade starch. Focus is on structures of new enzyme-types, new structures for previously characterized enzymes, and enzyme complexes with substrates, substrate analogues, natural products, and proteinaceous inhibitors. Starch-degrading enzymes according to CAZy [1] are found in GH families 3, 13, 14, 15, 31, 57, 119, eventually 126, auxiliary activities (AA) family 13 and GT family 35. α-amylases, α-glucosidases, limit dextrinases/pullulanases, isoamylases, lytic polysaccharide monooxygenases, disproportionating enzymes, and starch phosphorylases will be explicitly addressed (see Table 1 for a complete overview). α-glucan phosphatase is reviewed elsewhere in this issue [3].

The mentioned enzymes differ in catalytic domain fold, catalytic mechanism, and modular architecture encompassing auxiliary domains, primarily functionally and structurally discrete non-catalytic carbohydrate binding modules (CBMs) (Figure 2). Enzymes of the same family, e.g. GH13, can possess differently shaped active sites; i) a single shallow cleft spanning from a few to more than 10 glucosyl residues accommodating subsites for linear substrates in endo-acting α-amylases; ii) a pocket shaped binding site extending in exo-glucanases and glucosidases from a catalytic site in a deep cavity and composed of two to several subsites; or iii) in debranching enzymes two interconnected shallow clefts running in parallel.

Many of these multi-domain enzymes also contain dedicated carbohydrate binding sites that are situated outside of the active site area as seen for example on CBMs. Starch binding CBMs are organised in 12 families (CBM 20, 21, 25, 26, 34, 41, 45, 48, 53, 58, 68, 69; [1]). *In silico* "domain-walking" using a predicted CBM may disclose starch-active catalytic domains in full length sequences as in case of LPMOs in family AA13 [4] for which a crystal structure was recently solved [5]. Carbohydrate binding areas are also identified in form of surface surface binding sites (SBSs) situated on catalytic or intimately associated domains (Figure 2). Identification and functional characterisation of SBSs typically start with its observation in an enzyme:carbohydrate complex [6]. SBSs are difficult to predict even though several starch-active enzymes contain SBSs with validated roles in activity [7]. Recently, SBSs were also characterised in starch synthase I [8,9] and in glycogen synthase [10,11], where they ensure enzyme proximity to the α-glucan molecule during its elongation. SBSs have also been identified in α-glucan phosphatases (reviewed in [3]).

α-amylases

According to CAZy, α-amylase (EC 3.2.1.1), probably the best studied amylolytic enzyme, is found in GH13, GH57, GH119, and GH126 (α-amylase activity not fully confirmed) [1,12]. Eleven GH13 subfamilies contain α-amylases: GH13_1 (fungi), GH13_5 (bacterial liquefying enzymes), GH13_6 (plants), GH13_7 (archaea), GH13_15 (insects), GH13_24 (animals), GH13_27 (proteobacteria), GH13_28 (bacterial saccharifying enzymes), GH13_32 (bacteria), GH13_36 (intermediary α-amylase group evolutionary found between oligo-1,6-glucosidases and neopullulanases), GH13_37 (marine bacteria), and GH13_41 (starch degrading enzymes with both an α-amylase and a pullulanase domain [13]) [12,14]. Twenty-three different α-amylases are structure-determined including enzymes from GH13_5, GH13_6, and GH57 published recently [1,15–17]. The industrial GH13_5 *Bacillus* and *Geobacillus* α-amylases (known as 'Termamyl'-like α-amylases after the trade name of a *Bacillus licheniformis* enzyme) are represented by several structures [18–24], the newest being of an engineered variant of *Geobacillus stearothermophilus* GH13_5 α-amylase (PDB: 4UZU; parent PDB: 1HVX [20]) showing a tighter turning loop due to a two-residue truncation in the three-domain fold stabilised by Ca^{2+} and the Ca^{2+}–Na^{+}–Ca^{2+} triad of Termamyl-like α-amylases and a sodium ion mimicking the substrate transition-state charge (Figure 2a) [15]. The GH13_6 α-amylases are represented by structures of SBS-containing barley (*Hordeum vulgare*) isozymes 1 [25–28] and 2 [29,30], and the *N*-glycosylated rice (*Oryza sativa*) α-amylase AmyI-1 (PDB: 3WN6) that acts at an early stage of seed germination as well as in leaves and has

tartaric acid from the crystallisation binding at an SBS conserved in barley α-amylase (Figure 2b) [16]. Mutations of this SBS impeded AmyI-1 plastid targeting [31].

A structure-determined *Anoxybacillus* α-amylase (Table 1; Figure 2c) was proposed to form a new GH13 subfamily with α-amylases from thermophilic *Geobacillus* and a halophilic *Bacillus* species [32,33]. Maltose is the predominant starch hydrolysis product of these enzymes [34] and comparison of their structures (PDB: 4E2O) [35] revealed four well-ordered Ca^{2+} binding sites in *Anoxybacillus* α-amylase of which the *Geobacillus* enzymes only contains the two. Substrate interactions were maintained at subsites −2, −1, and +1, but observed conformational changes involved two conserved tryptophans and a loop to accommodate substrate at subsite + 2 that might alternatively connect to an additional subsite + 3 with a different ligand binding mode in the *Anoxybacillus* structure [33].

In addition to classical endo- and exo-acting α-amylases a number of enzymes (known as maltogenic amylases) have dual α-1,4-/α-1,6-linkage specificity. The structure of such a maltose-forming enzyme from *Pyrococcus* sp. ST04 with α-1,6-bond preference (PDB: 4CMR) [17] is assigned to GH57 in the literature, while CAZy states its GH family as “non-classified” [1]. It primarily recognizes and releases non-reducing-end maltose units from shorter linear oligosaccharides, distinct from endo-1,4-acting α-amylases, and the bond-type specificity has been altered by structure guided site-directed mutagenesis. The enzyme is tetrameric with a distinct substrate-binding channel extending from the active site placed in a small enclosed cavity towards the central hole of the tetramer (Figure 2d), making it structurally different from classical maltogenic amylases and β-amylases. A barrier adjacent to subsite −2 explains the novel action pattern [17].

α-glucosidase

GH families 4, 13, 31, 63, 97, and 122 contain α-glucosidases hydrolysing α-1,4-linkages in mainly maltose and short maltooligosaccharides with release of glucose from non-reducing ends [36]. The structure-determined GH13 α-glucosidase from *Halomonas* sp. H11 shows high activity only on maltose [37] and the enzyme:maltose complex (PDB: 3WY4; Figure 2e) unveils a peculiar long β–>α loop 4 responsible for strict disaccharide recognition by steric hindrance [37]. By contrast, most plant GH31 α-glucosidases prefer long maltooligosaccharides [36], sugar beet α-glucosidase (SBG) exhibiting 50- and 90-fold higher catalytic efficiency for maltoheptaose and soluble starch, respectively, than for maltose [38]. Some plant α-glucosidases, however, prefer di- and

trisaccharides like barley α-glucosidase [39]. Despite differences in substrate preference plant α-glucosidases of GH31 have significantly similar amino acid sequences [36]. Structures are available of several GH31 α-glucosidases [1], but only recently a plant α-glucosidase (SBG) was solved including bound 4–10 residues long acarviosyl-maltooligosaccharide inhibitors, considered as transition state mimics (Table 1; Figure 2f). These complexes revealed the structural basis of substrate specificity [36,40], illustrating how self-stabilization by long-chain amylose in a single-helical conformation is utilized in formation of enzyme-substrate complexes with remote subsites accommodating substrate largely *via* van der Waals interactions [40].

Starch debranching enzymes; limit dextrinase, pullulanases and isoamylases

Plant limit dextrinases and the closely related bacterial type I pullulanases hydrolysing α-1,6-linkages in pullulan, amylopectin and branched maltooligosaccharides (limit dextrins, hence the enzyme name) belong to subfamily GH13_13 with bacterial pullulanases, also found in GH13_12 and GH13_14, while isoamylases are in subfamily GH13_11. In addition to the classical pullulanase type I debranching enzymes, some organisms have type II pullulanases, which hydrolyze both α-1,4- and α-1,6-linkages in starch. This activity occurs in GH13 and GH57, but no structures are available. Starch debranching enzymes and their structures were recently reviewed [13].

The structures of plant (barley) limit dextrinase (LD) [41,42] were supplemented recently with an active site mutant in complex with limit dextrin (Figure 2g) – a branched maltohexaose with three glucose residues in both the main chain and the branch (PDB: 4J3W), providing the first structure of a debranching enzyme:substrate complex [43]. This and more LD structures containing substrates, products and substrate analogues (Table 1) contribute with new insight into substrate interactions of pullulanase type I debranching enzymes and propose main chain binding subsites to have high affinity and keep α-1,4-linkages away from the catalytic site whilst positioning the α-1,6-linkage for hydrolysis [43]. The topology of the active site and its surroundings was concluded to cause differences in substrate preferences and catalytic efficiencies of debranching enzymes [43].

Recent structures of a pullulanase type I from *Anoxybacillus* resulted in classification of the new CBM68 [44] and two structures (PDB: 3WDI and 3WDJ) showed two maltooligosaccharides parallelly accommodated close to each other between CBM68 and the catalytic domain (Figure 2h).

Isoamylases do not hydrolyse pullulan and have been hypothesised to trim misplaced branches in amylopectin during starch biosynthesis otherwise preventing adjacent linear chains from associating

and crystallizing [45–47]. Structures of free and maltoheptaose-complexed isoamylase from *Chlamydomonas reinhardtii* (Table 1) show details of the branch binding that rationalized low activity on tightly spaced branches [48]. Moreover, the isoamylase structure unveiled carbohydrate occupying an SBS located at the reducing-end binding area of the active site and a second SBS at the interface of the catalytic and C-terminal domains (Figure 2i) [48].

Lytic polysaccharide monooxygenases

Lytic polysaccharide monooxygenases (LPMOs) are copper-dependent and utilise molecular oxygen and an electron donor to cleave glucosidic bonds as demonstrated in cellulose, hemicellulose, chitin, or starch. Details on structure and function of LPMOs have been reviewed recently [49,50]. LPMOs acting on chitin [51] and crystalline cellulose [52] defined CAZy families AA9, AA10 and AA11 of enzymes having auxiliary activities, i.e. redox enzymes that act in conjunction with other CAZymes. Recently *Neurospora crassa* LPMO active on recalcitrant/retrograded starch [4] was assigned into family AA13 comprising 14 fungal members [1]. Genomic identification by CBM20 "module-walking" identified AA13 LPMO in *Aspergillus nidulans* and an *Aspergillus oryzae* orthologue lacking this SBD whose structure was determined (PDB: 4OPB) [5]. Remarkably, this structure has a shallow groove leading to the histidine-brace copper active site area (Figure 2j) as opposed to the flat active site surface in the three other LPMO AA families. Possibly this AA13 topology accommodates retrograded starch having a more irregularly shaped surface than crystalline cellulose and chitin [5].

Degradation of transitory starch

Degradation of transitory starch in plants during night involves a suite of enzyme activities, including glucan water dikinase, phosphoglucan water dikinase, SEX4 glucan phosphate phosphatase, β-amylase and isoamylase [53]. However, maltooligosaccharides of less than four glucose units are not substrates for these enzymes, maltotriose is therefore accumulating as only glucose and maltose are exported from the plastid. In plants the problem is circumvented by disproportionating enzyme 1 (DPE1) from GH77 converting two molecules of maltotriose to glucose and maltopentaose in turn attacked by β-amylase or starch phosphorylase to yield glucose and maltose that are exportable (Figure 1b). Several structures are available of DPE1 bacterial counterparts, including *Escherichia coli* MalQ [54]; a ligand-free potato structure was also reported (PDB: 1X1N; no literature reference). The structure of *Arabidopsis* DPE1 is solved in complex with

different ligands (Table 1) including maltononaose (Figure 2k), a disproportionation product of a maltotriose soak [55]. Six substrate complexes reveal a series of mechanistically relevant stages with a number of loops around the active site adopting different conformations governed by occupancy of certain subsites defining a complete catalytic cycle of DPE1 [55]. Similar conformational changes depending on substrate length were at the same time reported for MalQ [54].

A structure was also solved recently of *Arabidopsis* α-1,4-glucan phosphorylase AtPHS2 (PDB: 4BQE) that succeeds DPE1 in the degradation pathway [56] and structurally resembles the well-studied orthologue glycogen phosphorylase (GP) for which allosteric and covalent control were described [57,58]. Remotely relative to the active site AtPHS2 has maltotriose bound at a characteristic SBS not seen in GP, which is situated adjacent to and almost contiguous with the maltopentaose binding site of GP (PDB: 1P29). AtPHS2 is a biologically relevant dimer showing no interaction equivalent to GP with an allosteric activator and has a more open active site that may explain the lack of allosteric regulation [56].

Inhibitors of starch modifying enzymes

Human salivary (HSA) and pancreatic α-amylases (HPA), associated with carbohydrate uptake and thereby with diseases like diabetes and metabolic syndrome, are key inhibitor discovery targets [59,60]. A large number of structures are available of these enzymes, HPA first solved in 1995 (PDB: 1HNY) [61] and HSA in 1996 (PDB: 1SMD) [62]. Recently, a structure was determined of HPA in complex with the potent and specific inhibitor montbretin A (PDB: 4W93) (Figure 3a), a plant flavonol glycoside with potential in diabetes and obesity therapies [59]. Montbretin A applies a novel interaction mode where its two phenolic groups, myricetin and caffeic acid, are preorganised *via* hydrophobic stacking to optimize hydrogen bonding with the catalytic carboxyl groups (Figure 3a). The phenolic moieties are linked through a largely non-interacting disaccharide and a combination of structural studies and degradation analysis led to design of a simplified analogue in which they are connected *via* an alkyl chain [59]. Another structure of an HPA inhibitor was published in the beginning of 2016 (PDB: 4X0N). A high-throughput screen of marine natural product extracts identified a potent (K_i=10 pM) peptidic inhibitor, helianthamide. However, a complex of the inhibitor was only obtained with porcine pancreatic α-amylase (Figure 3b) that has high sequence and structural homology to HPA. Helianthamide belongs to a group of antimicrobial

peptides adopting a β-defensin fold and binds into and across the amylase active site (Figure 3b) [60] showing the first structure of a novel class of glycosidase inhibitors.

Control of starch degrading enzymes is also highly relevant for other organisms. Thus some plants use inhibitors in defence against pests as seen by the structure of a cereal-type inhibitor RBI (*Ragi* bifunctional α-amylase/trypsin inhibitor) in complex with an insect α-amylase from yellow mealworm (*Tenebrio molitor*) (PDB: 1TMQ) [63]. The barley LD is regulated by an endogenous limit dextrinase inhibitor (LDI) with picomolar affinity and the LD:LDI structure was solved recently (PDB: 4CVW; Figure 3c) [64]. LDI is also a cereal-type inhibitor, but with a role in controlling LD activity rather than in pest defence [64]. Remarkably, although LDI belongs to the cereal-type inihibitor family it uses a fundamentally different orientation in binding (Figure 3d) and has a unique motif that stabilizes the enzyme complex through an intermolecular hydrophobic cluster (Figure 3c). The LDI and helianthamide enzyme complexes add to the five previously described modes of proteinaceous inhibitor GH13 starch-hydrolase interactions [65].

Conclusions

New details on functional structural elements add to understanding of mechanism of action and specificity of enzymes participating in starch-degradation. Notable advances concern complexes containing branched or long oligosaccharide substrates/inhibitory substrate analogues enlightening enzyme structural elements engaged in macromolecular substrate interactions. Overall new structural facets offer targets for innovative protein engineering exploiting and unravelling relationships between structure and function in the enzyme-substrate/inhibitor interplays.

Acknowledgements

This work was supported by The Danish Council for Independent Research | Technology and Production Sciences, including a Sapere Aude-Research Talent grant (to MSM), and | Natural Sciences (to BS).

References

1. Lombard V, Golaconda Ramulu H, Drula E, Coutinho PM, Henrissat B: **The carbohydrate-active enzymes database (CAZy) in 2013**. *Nucleic Acids Res.* 2014, **42**:490–495.
2. Vamadevan V, Bertoft E: **Structure-function relationships of starch components**. *Starch - Stärke* 2015, **67**:55–68.
3. Gentry MS: **The structural biology of glucan phosphatases**. *Curr. Opin. Struct. Biol.* 2016, **40 Carbohy**.
4. Vu V V, Beeson WT, Span EA, Farquhar ER, Marletta MA: **A family of starch-active polysaccharide monooxygenases.** *Proc. Natl. Acad. Sci. U. S. A.* 2014, **111**:13822–7.
   (•) Discovery and characterization of starch-active LPMO subsequently assigned into AA13.
5. Lo Leggio L, Simmons TJ, Poulsen J-CN, Frandsen KEH, Hemsworth GR, Stringer MA, von Freiesleben P, Tovborg M, Johansen KS, De Maria L, et al.: **Structure and boosting activity of a starch-degrading lytic polysaccharide monooxygenase.** *Nat. Commun.* 2015, **6**:5961.
   (••) First crystal structure of a starch-active LPMO, a representative of the new AA13 family showing a shallow groove leading to the active site.
6. Cockburn D, Wilkens C, Ruzanski C, Andersen S, Willum Nielsen J, Smith A, Field R, Willemoës M, Abou Hachem M, Svensson B: **Analysis of surface binding sites (SBSs) in carbohydrate active enzymes with focus on glycoside hydrolase families 13 and 77 — a mini-review**. *Biologia (Bratisl).* 2014, **69**:705–712.
7. Cockburn D, Nielsen MM, Christiansen C, Andersen JM, Rannes JB, Blennow A, Svensson B: **Surface binding sites in amylase have distinct roles in recognition of starch structure motifs and degradation**. *Int. J. Biol. Macromol.* 2015, **75**:338–345.
8. Cuesta-Seijo JA, Nielsen MM, Marri L, Tanaka H, Beeren SR, Palcic MM: **Structure of starch synthase I from barley: insight into regulatory mechanisms of starch synthase activity**. *Acta Crystallogr. Sect. D Biol. Crystallogr.* 2013, **69**:1013–1025.
9. Wilkens C, Cuesta-Seijo J a., Palcic M, Svensson B: **Selectivity of the surface binding site (SBS) on barley starch synthase I**. *Biologia (Bratisl).* 2014, **69**:1118–1121.
10. Baskaran S, Chikwana VM, Contreras CJ, Davis KD, Wilson WA, DePaoli-Roach AA, Roach PJ, Hurley TD: **Multiple glycogen-binding sites in eukaryotic glycogen synthase are required for high catalytic efficiency toward glycogen**. *J. Biol. Chem.* 2011, **286**:33999–34006.

11. Díaz A, Martínez-Pons C, Fita I, Ferrer JC, Guinovart JJ: **Processivity and subcellular localization of glycogen synthase depend on a non-catalytic high affinity glycogen-binding site**. *J. Biol. Chem.* 2011, **286**:18505–18514.
12. Janeček Š, Svensson B, MacGregor EA: **α-amylase: an enzyme specificity found in various families of glycoside hydrolases**. *Cell. Mol. Life Sci.* 2014, **71**:1149–1170.
13. Møller MS, Henriksen A, Svensson B: **Structure and function of α-glucan debranching enzymes**. *Cell. Mol. Life Sci.* 2016, **73**:2619–2641.
14. Stam MR, Danchin EGJ, Rancurel C, Coutinho PM, Henrissat B: **Dividing the large glycoside hydrolase family 13 into subfamilies: towards improved functional annotations of α-amylase-related proteins.** *Protein Eng. Des. Sel.* 2006, **19**:555–562.
15. Offen WA, Viksoe-Nielsen A, Borchert T V., Wilson KS, Davies GJ: **Three-dimensional structure of a variant `Termamyl-like' Geobacillus stearothermophilus α-amylase at 1.9 Å resolution**. *Acta Crystallogr. Sect. F Struct. Biol. Commun.* 2015, **71**:66–70.
16. Ochiai A, Sugai H, Harada K, Tanaka S, Ishiyama Y, Ito K, Tanaka T, Uchiumi T, Taniguchi M, Mitsui T: **Crystal structure of α-amylase from Oryza sativa: molecular insights into enzyme activity and thermostability**. *Biosci. Biotechnol. Biochem.* 2014, **78**:989–997.
(•) Crystal structure of rice α-amylase AmyI-1 a major isozyme in the scutellum epithelium and aleurone layers of the seeds during germination. On the $(\beta/\alpha)_8$-barrel catalytic domain an SBS present in barley α-amylase is conserved.
17. Park KH, Jung JH, Park SG, Lee ME, Holden JF, Park CS, Woo EJ: **Structural features underlying the selective cleavage of a novel exo-type maltose-forming amylase from *Pyrococcus* sp. ST04**. *Acta Crystallogr. Sect. D Biol. Crystallogr.* 2014, **70**:1659–1668.
(•) Crystal structure of a *Pyrococcus* exo-type maltose-forming amylase of family GH57 with preference for α-1,6-bonds and dual α-1,4-/α-1,6-bond specificity amenable to rational engineering.
18. Machius M, Declerck N, Huber R, Wiegand G: **Activation of Bacillus licheniformis α-amylase through a disorder→order transition of the substrate-binding site mediated by a calcium-sodium-calcium metal triad**. *Structure* 1998, **6**:281–292.
19. Brzozowski AM, Lawson DM, Turkenburg JP, Bisgaard-Frantzen H, Svendsen A, Borchert T V, Dauter Z, Wilson KS, Davies GJ: **Structural analysis of a chimeric bacterial α-amylase. High-resolution analysis of native and ligand complexes**. *Biochemistry* 2000, **39**:9099–9107.

20. Suvd D, Fujimoto Z, Takase K, Matsumura M, Mizuno H: **Crystal structure of *Bacillus stearothermophilus* α-amylase: possible factors determining thermostability**. *J. Biochem.* 2001, **129**:461–468.
21. Kanai R, Haga K, Akiba T, Yamane K, Harata K: **Biochemical and crystallographic analyses of maltohexaose-producing amylase from alkalophilic *Bacillus* sp. 707**. *Biochemistry* 2004, **43**:14047–14056.
22. Davies GJ, Marek Brzozowski A, Dauter Z, Rasmussen MD, Borchert T V., Wilson KS: **Structure of a *Bacillus halmapalus* family 13 α-amylase, BHA, in complex with an acarbose-derived nonasaccharide at 2.1 Å resolution**. *Acta Crystallogr. Sect. D Biol. Crystallogr.* 2005, **61**:190–193.
23. Shirai T, Igarashi K, Ozawa T, Hagihara H, Kobayashi T, Ozaki K, Ito S: **Ancestral sequence evolutionary trace and crystal structure analyses of alkaline α-amylase from Bacillus sp. KSM-1378 to clarify the alkaline adaptation process of proteins**. *Proteins Struct. Funct. Bioinforma.* 2007, **66**:600–610.
24. Alikhajeh J, Khajeh K, Ranjbar B, Naderi-Manesh H, Lin YH, Liu E, Guan HH, Hsieh YC, Chuankhayan P, Huang YC, et al.: **Structure of *Bacillus amyloliquefaciens* α-amylase at high resolution: Implications for thermal stability**. *Acta Crystallogr. Sect. F Struct. Biol. Cryst. Commun.* 2010, **66**:121–129.
25. Robert X, Haser R, Gottschalk T, Ratajczak F, Driguez H, Svensson B, Aghajari N: **The structure of barley α-amylase isozyme 1 reveals a novel role of domain C in substrate recognition and binding: A pair of sugar tongs**. *Structure* 2003, **11**:973–984.
26. Robert X, Haser R, Mori H, Svensson B, Aghajari N: **Oligosaccharide binding to barley α-amylase 1**. *J. Biol. Chem.* 2005, **280**:32968–78.
27. Bozonnet S, Jensen MT, Nielsen MM, Aghajari N, Jensen MH, Kramhøft B, Willemoës M, Tranier S, Haser R, Svensson B: **The "pair of sugar tongs" site on the non-catalytic domain C of barley α-amylase participates in substrate binding and activity**. *FEBS J.* 2007, **274**:5055–5067.
28. Nielsen MM, Seo ES, Bozonnet S, Aghajari N, Robert X, Haser R, Svensson B: **Multi-site substrate binding and interplay in barley α-amylase 1**. *FEBS Lett.* 2008, **582**:2567–2571.
29. Kadziola A, Abe J, Svensson B, Haser R: **Crystal and molecular structure of barley α-amylase**. *J. Mol. Biol.* 1994, **239**:104–121.
30. Kadziola A, Søgaard M, Svensson B, Haser R: **Molecular structure of a barley α-amylase-**

inhibitor complex: implications for starch binding and catalysis. *J. Mol. Biol.* 1998, **278**:205–217.

31. Kitajima A, Asatsuma S, Okada H, Hamada Y, Kaneko K, Nanjo Y, Kawagoe Y, Toyooka K, Matsuoka K, Takeuchi M, et al.: **The rice α-amylase glycoprotein is targeted from the Golgi apparatus through the secretory pathway to the plastids**. *Plant Cell* 2009, **21**:2844–2858.
32. Ranjani V, Janeček S, Chai KP, Shahir S, Abdul Rahman RNZR, Chan K-G, Goh KM: **Protein engineering of selected residues from conserved sequence regions of a novel Anoxybacillus α-amylase**. *Sci. Rep.* 2014, **4**:5850–5858.
33. Chai KP, Othman NFB, Teh A-H, Ho KL, Chan K-G, Shamsir MS, Goh KM, Ng CL: **Crystal structure of *Anoxybacillus* α-amylase provides insights into maltose binding of a new glycosyl hydrolase subclass**. *Sci. Rep.* 2016, **6**:23126.
34. Chai YY, Rahman RNZRA, Illias RM, Goh KM: **Cloning and characterization of two new thermostable and alkalitolerant α-amylases from the *Anoxybacillus* species that produce high levels of maltose**. *J. Ind. Microbiol. Biotechnol.* 2012, **39**:731–741.
35. Mok SC, Teh AH, Saito JA, Najimudin N, Alam M: **Crystal structure of a compact α-amylase from *Geobacillus thermoleovorans***. *Enzyme Microb. Technol.* 2013, **53**:46–54.
36. Tagami T, Yamashita K, Okuyama M, Mori H, Yao M, Kimura A: **Molecular basis for the recognition of long-chain substrates by plant α-glucosidases**. *J. Biol. Chem.* 2013, **288**:19296–19303.
37. Shen X, Saburi W, Gai Z, Kato K, Ojima-Kato T, Yu J, Komoda K, Kido Y, Matsui H, Mori H, et al.: **Structural analysis of the α-glucosidase HaG provides new insights into substrate specificity and catalytic mechanism**. *Acta Crystallogr. Sect. D Biol. Crystallogr.* 2015, **71**:1382–1391.

    (•) Based on steric hindrance provided by a long β–>α 4 loop of the $(\beta/\alpha)_8$-barrel catalytic domain this GH13 α-glucosidase showed strict disaccharide specificity.
38. Matsui H, Chiba S, Shimomura T: **Substrate specificity of an α-glucosidase in sugar beet seeds**. *Agric. Biol. Chem.* 1978, **42**:1855–1860.
39. Im H, Henson CA: **Characterization of high pI α-glucosidase from germinated barley seeds: substrate specificity, subsite affinities and active-site residues**. *Carbohydr. Res.* 1995, **277**:145–159.
40. Tagami T, Yamashita K, Okuyama M, Mori H, Yao M, Kimura A: **Structural advantage of**

sugar beet α-glucosidase to stabilize the Michaelis complex with long-chain substrate. *J. Biol. Chem.* 2015, **290**:1796–1803.

(••) Crystal structure of sugar beet GH31 α-glucosidase in complex with acarviosyl-maltooligosaccharides accommodated at the active site and *via* substrate self-stabilisation contributing to the interaction in particular with distant subsites.

41. Vester-Christensen MB, Abou Hachem M, Svensson B, Henriksen A: **Crystal structure of an essential enzyme in seed starch degradation: barley limit dextrinase in complex with cyclodextrins.** *J. Mol. Biol.* 2010, **403**:739–50.
42. Møller MS, Abou Hachem M, Svensson B, Henriksen A: **Structure of the starch-debranching enzyme barley limit dextrinase reveals homology of the N-terminal domain to CBM21.** *Acta Crystallogr. Sect. F. Struct. Biol. Cryst. Commun.* 2012, **68**:1008–12.
43. Møller MS, Windahl MS, Sim L, Bøjstrup M, Abou Hachem M, Hindsgaul O, Palcic M, Svensson B, Henriksen A: **Oligosaccharide and substrate binding in the starch debranching enzyme barley limit dextrinase**. *J. Mol. Biol.* 2015, **427**:1263–1277.

(••) Crystal structure of a catalytic residue mutated debranching enzyme in the first complex with a natural limit dextrin substrate.

44. Xu J, Ren F, Huang C-H, Zheng Y, Zhen J, Sun H, Ko T-P, He M, Chen C-C, Chan H-C, et al.: **Functional and structural studies of pullulanase from Anoxybacillus sp. LM18-11**. *Proteins Struct. Funct. Bioinforma.* 2014, **82**:1685–1693.

(••) Crystal structure of a remarkably thermostable pullulanase in complex with two oligosaccharides at the catalytic domain in parallel binding mode and another interacting with the N-terminal starch binding family CBM68 domain.

45. Nakamura Y: **Towards a better understanding of the metabolic system for amylopectin biosynthesis in plants: rice endosperm as a model tissue.** *Plant Cell Physiol.* 2002, **43**:718–25.
46. Myers AM, Morell MK, James MG, Ball SG: **Update on biochemistry recent progress toward understanding biosynthesis of the amylopectin crystal**. *Plant Physiol.* 2000, **122**:989–997.
47. Jeon J-S, Ryoo N, Hahn T-R, Walia H, Nakamura Y: **Starch biosynthesis in cereal endosperm.** *Plant Physiol. Biochem.* 2010, **48**:383–92.
48. Sim L, Beeren SR, Findinier J, Dauvillée D, Ball S, Henriksen A, Palcic MM: **Crystal**

structure of the Chlamydomonas starch debranching enzyme isoamylase ISA1 reveals insights into the mechanism of branch trimming and complex assembly. *J. Biol. Chem.* 2014, **289**:22991–23003.

(••) Crystal structure of isoamylase in complex with maltoheptaose revealing details about the mechanism of branch binding, suggesting a role in trimming of misplaced branches during amylopectin synthesis, and containing two surface binding sites.

49. Span EA, Marletta MA: **The framework of polysaccharide monooxygenase structure and chemistry**. *Curr. Opin. Struct. Biol.* 2015, **35**:93–99.
50. Vu V V, Marletta MA: **Starch-degrading polysaccharide monooxygenases**. *Cell. Mol. Life Sci.* 2016, **73**:2809–2819.
51. Vaaje-Kolstad G, Westereng B, Horn SJ, Liu Z, Zhai H, Sørlie M, Eijsink VGH: **An oxidative enzyme boosting the enzymatic conversion of recalcitrant polysaccharides**. *Science.* 2010, **330**:219–222.
52. Harris P V., Welner D, McFarland KC, Re E, Navarro Poulsen JC, Brown K, Salbo R, Ding H, Vlasenko E, Merino S, et al.: **Stimulation of lignocellulosic biomass hydrolysis by proteins of glycoside hydrolase family 61: Structure and function of a large, enigmatic family**. *Biochemistry* 2010, **49**:3305–3316.
53. Smith AM: **Starch in the Arabidopsis plant**. *Starch - Stärke* 2012, **64**:421–434.
54. Weiss SC, Skerra A, Schiefner A: **Structural basis for the interconversion of maltodextrins by MalQ, the amylomaltase of *Escherichia coli***. *J. Biol. Chem.* 2015, **290**:21352–21364.
55. O'Neill EC, Stevenson CEM, Tantanarat K, Latousakis D, Donaldson MI, Rejzek M, Nepogodiev SA, Limpaseni T, Field RA, Lawson DM: **Structural dissection of the maltodextrin disproportionation cycle of the Arabidopsis plastidial enzyme DPE1**. *J. Biol. Chem.* 2015, **290**:29834–29853.

(••) Crystal structures of DPE1 plastidial disproportionating enzyme in complex with different ligands are trapped in conformational states that allow definition of a structural basis for the catalytic mechanism.

56. O'Neill EC, Rashid AM, Stevenson CEM, Hetru A-C, Gunning AP, Rejzek M, Nepogodiev SA, Bornemann S, Lawson DM, Field RA: **Sugar-coated sensor chip and nanoparticle surfaces for the in vitro enzymatic synthesis of starch-like materials**. *Chem. Sci.* 2014, **5**:341–350.

(•) Crystal structure of the *Arabidopsis* phosphorylase AtPHS2 in complex with maltotriose and acarbose bound at the surface of the enzyme.

57. Barford D, Hu S-H, Johnson LN: **Structural mechanism for glycogen-phosphorylase control by phosphorylation and AMP**. *J. Mol. Biol.* 1991, **218**:233–260.

58. Buchbinder JL, Rath VL, Fletterick RJ: **Structural relationships among regulated and unregulated phosphorylases.** *Annu. Rev. Biophys. Biomol. Struct.* 2001, **30**:191–209.

59. Williams LK, Zhang X, Caner S, Tysoe C, Nguyen NT, Wicki J, Williams DE, Coleman J, McNeill JH, Yuen V, et al.: **The amylase inhibitor montbretin A reveals a new glycosidase inhibition motif**. *Nat. Chem. Biol.* 2015, **11**:691–696.
(•) Crystal structure of human pancreatic α-amylase in complex with the flavonol glycoside potent inhibitor montbretin A reveals a new inhibitor motif where caffeine and myrecitin phenolics interact resulting in hydrogen bond formation with catalytic acids.

60. Tysoe C, Williams LK, Keyzers R, Nguyen NT, Tarling C, Wicki J, Goddard-Borger ED, Aguda AH, Perry S, Foster LJ, et al.: **Potent human α-amylase inhibition by the β-defensin-like protein helianthamide**. *ACS Cent. Sci.* 2016, **2**:154–161.
(•) Crystal structure of porcine pancreatic α-amylase in a high affinity complex with helianthamide, representing a new type of complex formation with a antimicrobial β-defensin fold being non-immunogenic and having high stability as opposed to other high affinity peptide and proteinaceous inhibitors.

61. Brayer GD, Luo Y, Withers SG: **The structure of human pancreatic α-amylase at 1.8 Å resolution and comparisons with related enzymes**. *Protein Sci.* 1995, **4**:1730–1742.

62. Ramasubbu N, Paloth V, Luo Y, Brayer GD, Levine MJ: **Structure of human salivary α-amylase at 1.6 Å resolution: Implications for its role in the oral cavity**. *Acta Crystallogr. Sect. D Biol. Crystallogr.* 1996, **52**:435–446.

63. Strobl S, Maskos K, Wiegand G, Huber R, Gomis-Rüth FX, Glockshuber R: **A novel strategy for inhibition of α-amylases: yellow meal worm α-amylase in complex with the Ragi bifunctional inhibitor at 2.5 Å resolution**. *Structure* 1998, **6**:911–921.

64. Møller MS, Vester-Christensen MB, Jensen JM, Abou Hachem M, Henriksen A, Svensson B: **Crystal structure of barley limit dextrinase-limit dextrinase inhibitor (LD-LDI) complex reveals insights into mechanism and diversity of cereal-type inhibitors**. *J. Biol. Chem.* 2015, **290**:12614–12629.
(••) Crystal structure of the complex of debranching limit dextrinase in complex with an

endogenous inhibitor of the cereal-inhibitor family that applies a unique binding mode stabilized by an intermolecular hydrophobic cluster formed adjacent to the catalytic site.

65. Svensson B, Fukuda K, Nielsen PK, Bønsager BC: **Proteinaceous α-amylase inhibitors.** *Biochim. Biophys. Acta* 2004, **1696**:145–56.

66. Mikami B, Iwamoto H, Malle D, Yoon H-J, Demirkan-Sarikaya E, Mezaki Y, Katsuya Y: **Crystal structure of pullulanase: evidence for parallel binding of oligosaccharides in the active site.** *J. Mol. Biol.* 2006, **359**:690–707.

67. Davies GJ, Wilson KS, Henrissat B: **Nomenclature for sugar-binding subsites in glycosyl hydrolases**. *Biochem. J. Lett.* 1997, **321**:557–559.

Tables

Table 1. Overview of the recent structures of starch degrading enzymes covered in the present review.

Enzyme type	Organism	PDB	Ligand (s) bound	Reso-lution (Å)	References
α-amylase (GH13_5)	*Geobacillus stearothermophilus*	4UZU	None	1.90	[15]
α-amylase I-1 (GH13_6)	*Oryza sativa Japonica* gr., rice	3WN6	None	2.16	[16]
Isoamylase (GH13_11)	*Chlamydomonas reinhardtii*	4J7R 4OKD	None Maltoheptaose	2.3 2.4	[48]
Limit dextrinase (GH13_13)	*Hordeum vulgare*, barley	4CVW 4J3S 4J3T 4J3U 4J3V 4J3W 4J3X	Proteinaceous inhibitor Maltotriose+maltotetraose Maltotetraose Maltosyl-S-β-cyclodextrin Branched thio-linked hexasaccharide Amylopectin fragment Pullulan fragment	2.67 1.75 1.6 1.7 1.45 1.67 1.75	[43,64]
Pullulanase type I (GH13_14)	*Anoxybacillus* sp. LM18-11	3WDH 3WDI 3WDJ	None Maltotriose Maltotetraose	1.75 2.2 2.22	[44]
α-glucosidase (GH13_23)	*Halomonas* sp. H11	3WY1 3WY2 3WY3 3WY4	None Glucose Glucose and glycerol Maltose	2.15 1.47 3.00 2.50	[37]
α-amylase (GH13_no subfam)	*Anoxybacillus* sp. SK3-4	5A2A 5A2B 5A2C	None Maltose Maltotriose	1.95 1.85 1.90	[33]
α-glucosidase (GH31)	*Beta vulgaris*, sugar beet	3W38 3W37 3WEL 3WEM 3WEN 3WEO	None Acarbose Acarviosyl-maltotriose Acarviosyl-maltotetraose Acarviosyl-maltopentaose Acarviosyl-maltohexaose	2.79 1.7 1.84 2.59 2.59 1.45	[36,40]
Maltose-forming α-amylase (GH57)	*Pyrococcus* sp. ST04	4CMR	None	1.8	[17]
Dispropor-tionating enzyme 1 (GH77)	*Arabidopsis*	5CPQ 5CPS 5CPT 5CQ1 5CSU 5CSY	None Maltoctaose+maltononaose β-cyclodextrin Cycloamylose Ascarviostatin Acarbose	2.13 1.8 2.3 2.3 2.53 2.05	[55]
α-1,4-glucan phosphorylase (GT35)	*Arabidopsis*	4BQE 4BQF 4BQI	None Acarbose Maltotriose	1.70 2.35 1.90	[56]
Lytic polysaccharide monooxygenase (AA13)	*Aspergillus oryzae*	4OPB	None	1.5	[5]

Figure legends

Figure 1. Schematic overview of the activity of the starch-active enzymes reviewed. The glucose units (hexagons) of the linear maltooligosaccharides are connected by α-1,4-glucosidic linkages, while the branch points are α-1,6-linkages. The reducing ends are indicated by a grey hexagon. **(a)** Starch degradation in general and in particular in the germinating seed of cereals (the only starch debranching enzyme active is limit dextrinase). **(b)** Action of the disproportionating enzyme 1 and associated enzymes during degradation of transitory starch. **(c)** Schematic illustration of general subsite nomenclature for α-1,4-active enzymes (top) and debranching enzymes (bottom), where each subsite interacts with one glucosyl unit and the number of subsites can vary (adapted from [66,67]).

Figure 2. Starch degrading enzymes covered in the present review. The structures are colored according to domains: N-domain, green; CBM, red; catalytic domain, beige; C-domain, orange; other domains, yellow; catalytic residues, black spheres; Ca^{2+}, purple spheres; and ligands, cyan sticks or sphere representation. See Table 1 for literature references. **(a)** GH13_5 α-amylase from *Geobacillus stearothermophilus* (PDB: 4UZU) – the Ca^{2+}–Na^{+}–Ca^{2+} triad is encircled. **(b)** GH13_6 α-amylase from rice (PDB: 3WN6); with tartaric acid bound to the SBS (encircled). **(c)** *Anoxybacillus* α-amylase in complex with maltotriose (PDB: 5A2C). **(d)** The tetrameric GH57 α-amylase from *Pyrococcus* (PDB: 4CMR). One subunit is boxed. **(e)** GH13_23 α-glucosidase from *Halomonas* with its preferred substrate maltose bound in the deep and narrow active site (PDB: 3WY4). **(f)** The GH31 α-glucosidase from sugar beet with preference for longer oligosaccharides, here complexed with acarviosyl-maltohexaose (cyan spheres) (PDB: 3WEO). **(g)** Overall structure of barley limit dextrinase in complex with limit dextrin (PDB: 4J3W), i.e. an α-1,6-branched maltooligosaccharide (excerpt; α-1,6-linkage encircled and the catalytic residues shown as black sticks). **(h)** Binding of maltotetraose molecules to the active site as well as the CBM68 of the *Anoxybacillus* pullulanase (PDB: 3WDJ). **(i)** The dimeric structure of the isoamylase from *Chlamydomonas* (PDB: 4OKD), with the excerpt highlighting the binding of maltooligosaccharides to the active site as well as the two SBSs. **(j)** The starch degrading LPMO from *Aspergillus oryzae* (PDB: 4OPB) with the copper ion shown as orange sphere. **(k)** Dimeric DPE1 (one unit with surface and one shown as cartoon) in complex with maltononaose (PDB: 5CPS), a disproportionation product from the maltotriose soak. **(l)** Dimeric α-1,4-glucan phosphorylase with

maltotriose bound to an SBS, while and the deeply buried PLP cofactor is shown as pink spheres (PDB: 4BQI).

Figure 3. Overview of recent enzyme:inhibitor complex structures. Enzymes are beige, while inhibitors are orange, and the catalytic residues are shown as black sticks. **(a)** Overall structure of HPA in complex with the inhibitor montbretin A (PDB: 4W93), and a closer look at the interaction between two phenolic moieties of the inhibitor, myricetin and caffeic acid, and the α-amylase. The phenolic moieties are preorganised via hydrophobic stacking to optimize hydrogen bonding with the catalytic carboxyl groups. **(b)** The peptidic inhibitor, helianthamide, in complex with porcine pancreatic α-amylase (PDB: 4X0N), and a intercept of the structure showing the key residues for the binding. **(c)** Overall structure of the LD:LDI complex (PDB: 4CVW) with a closer look at the intermolecular hydrophobic cluster stabilizing the complex. **(d)** Superimposition of LDI (orange) and RBI (green) in complex with their targets, LD (beige; PDB: 4CVW) and yellow mealworm α-amylase (light blue; PDB: 1TMQ), respectively, highlighting the different binding modes.

α-amylase β-amylase α-glucosidase

Starch debranching enzyme
(Isoamylase/limit dextrinase/pullulanase)

Figure 1

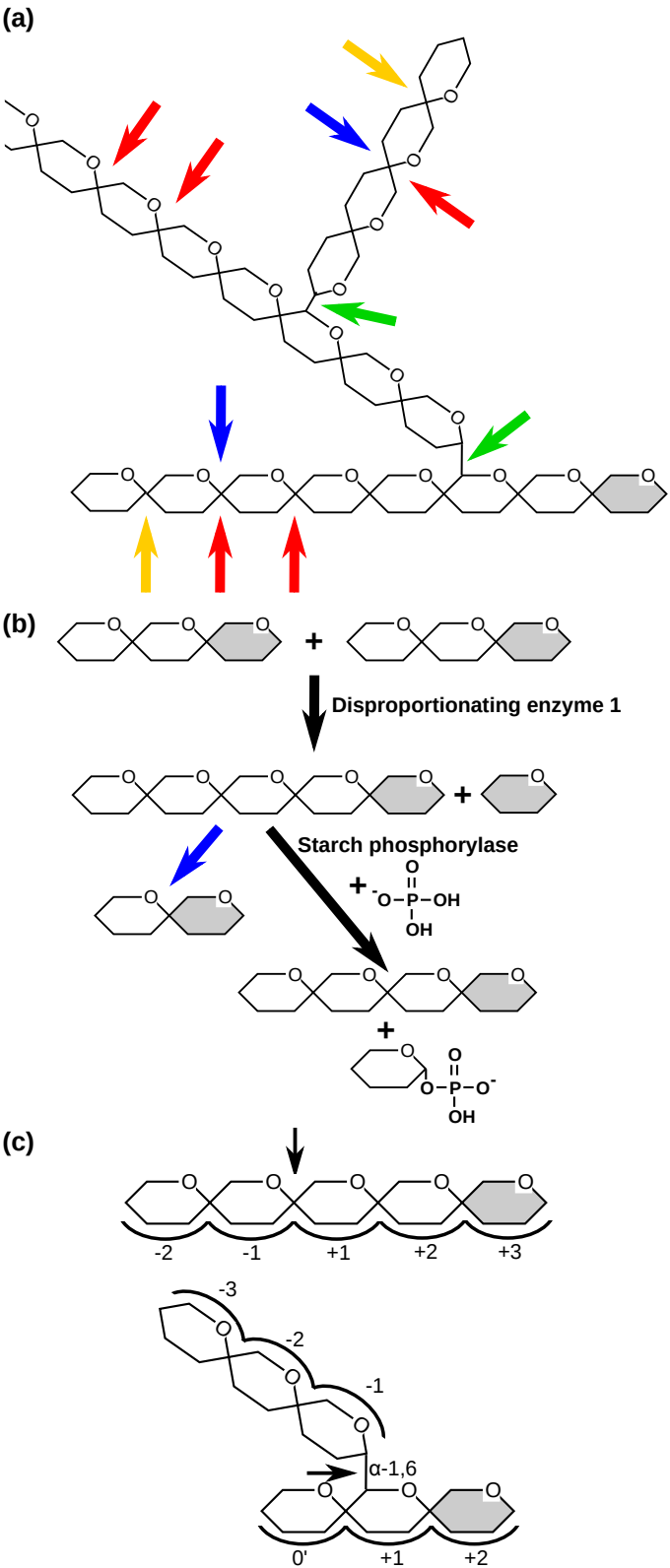

Figure 2

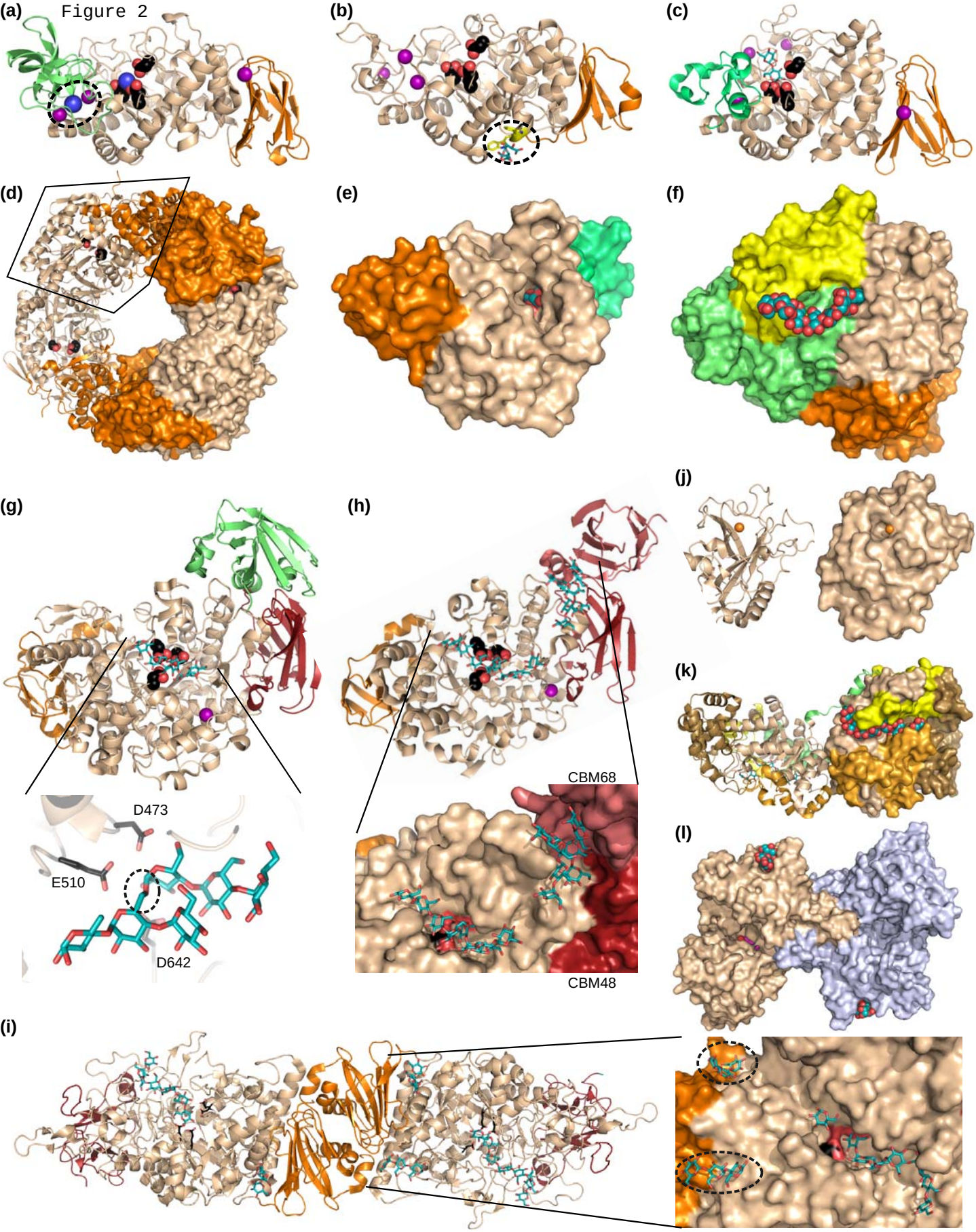

Figure 3

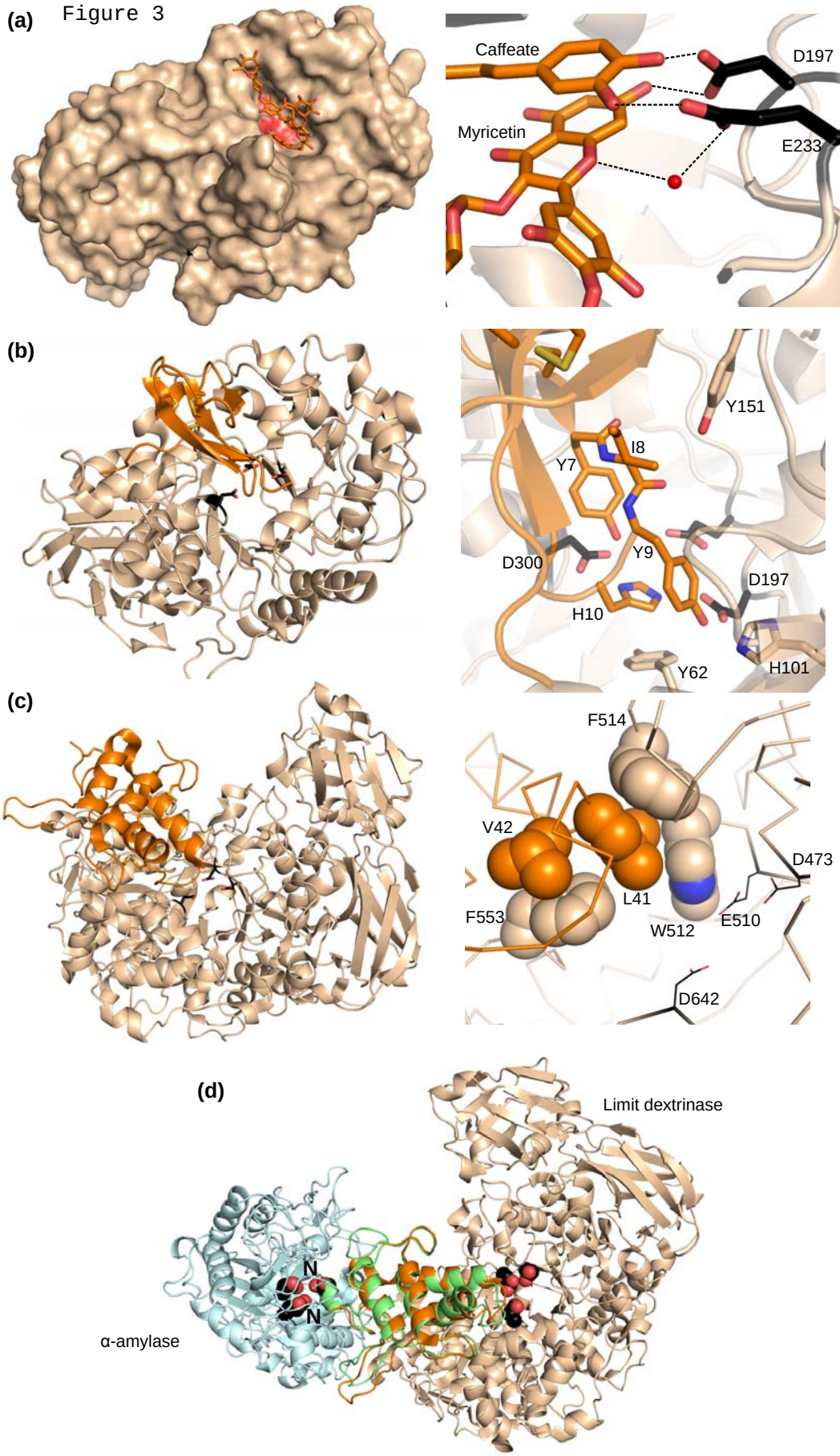
(a)
Caffeate
D197
Myricetin
E233
(b)
Y151
I8
Y7
Y9
D300
D197
H10
Y62
H101
(c)
F514
V42
D473
L41
F553
W512
E510
D642
(d)
Limit dextrinase
N
N
α-amylase